OFF-WALL BOUNDARY CONDITIONS FOR TURBULENT SIMULATIONS FROM MINIMAL FLOW UNITS IN TRANSITIONAL BOUNDARY LAYERS

Ricardo García-Mayoral
Center for Turbulence Research
Stanford University
Bldg. 500, Stanford, CA 94305, USA
gmayoral@stanford.edu

Brian Pierce
Center for Turbulence Research
Stanford University
Bldg. 500, Stanford, CA 94305, USA
bpierce1@stanford.edu

James M. Wallace
Burgers Program for Fluid Dynamics
University of Maryland
4247 CSS Bldg., College Park, MD 20742, USA
wallace@umd.edu

ABSTRACT

A reduced order model for off-wall boundary conditions for turbulent flows is proposed. The model circumvents the need to resolve the buffer layer near the wall by providing conditions directly above it for the overlying flow. The effect of the buffer layer is modeled as a pattern of periodic blocks similar to the minimal unit of Jiménez & Moin (1991). The model is reduced to the imprint of such blocks on a plane at $y^+ \approx 100$, at which Dirichlet boundary conditions are imposed for the rest of the flow. Blocks are constructed from a variety of canonical flows, from low-Reynolds-number turbulent channels to the transitional-boundary-layer direct simulation of Sayadi *et al.* (2012). The block sizes are selected so that they are statistically representative of fully turbulent flow, and so that they contain the dominant structures at $y^+ \approx 100$, as educed from direct mode decomposition. The model has the form of a collection of Fourier modes in space and time, and comprises ~1% of the parameters necessary to describe the full flow field at the plane considered, while it reproduces ~90% of the amplitudes of the flow statistics. The simulations conducted with these modeled off-wall boundary conditions correctly reproduce the turbulent statistics of the overlying flow.

INTRODUCTION

It has long been recognized that using sufficiently resolved large eddy simulations (LES) of bounded turbulent flows for typical engineering applications at high Reynolds numbers is impractical, given current and predicted future computing power. To address this problem, wall models have been proposed to avoid the need to extend the LES into the wall region, where the resolution of the small-scale eddies would require as much as 99% of the grid points in only about 10% of a flow with a Reynolds number based on an integral scale of order 10^6 (Piomelli & Balaras, 2002). The flow in the wall layer is often represented only in the average sense using the Reynolds averaged Navier-Stokes (RANS) equations or approximated by the thin turbulent boundary layer equations. Many of these wall models attempt, in various ways, to relate the wall stress, which LES cannot give accurately because of its insufficient grid resolution, to the outer flow in order to obtain boundary conditions for the computation. This subclass of wall models have been called wall stress models in a review by Cabot & Moin (1999).

An alternative described by Cabot & Moin (1999) is to use off-wall boundary conditions. In this case, the outer flow is computed by an LES with a grid providing sufficient and affordable resolution down to a chosen distance from the wall, and approximate boundary conditions are provided to the LES at that plane in the flow. In their review, Cabot and Moin cite attempts of this type by Bagwell *et al.* (1993), Balaras *et al.* (1996) and Nicoud *et al.* (1998) which they characterize as being largely unsuccessful because it appears that the relative phases and time scales of the underlying flow must be accurately represented in the off-wall boundary conditions. Furthermore, they also cite Jiménez & Vasco (1998) who observed that the wall layer flow is quite sensitive to the transpiration of the vertical velocity across the off-wall plane in order to maintain continuity.

A recent attempt to develop off-wall models is that of Chung & Pullin (2009) in an LES of a turbulent channel flow up to very high Reynolds numbers. They determine the slip velocity at an off-wall plane in the logarithmic region with the Karman constant calculated dynamically. This is done by relating the slip velocity to the shear stress at each location on the wall which, in turn, is calculated from an ODE obtained by wall-parallel filtering and wall-normal averaging of the streamwise momentum equation. What Chung and Pullin call an extended form of the stretched-vortex subgrid-scale (SGS) model is used to calculate a logarithmic relation at the off-wall location and thus the slip velocity.

In the present work, we investigate the possibility of reduced-order modeled off-wall boundary conditions for turbulent flows. Our objective is to model the effect of the buffer layer on the overlying flow as off-wall, Dirichlet boundary conditions. We select the plane at $y^+ \approx 100$ as our off-wall boundary, since this plane can be interpreted as a notional interface between the buffer and logarithmic regions. The underlying assumption is that the turbulent cycle in the log layer is essentially independent of the buffer region (Mizuno & Jiménez, 2013), and that the former does not require the actual presence of the latter to sustain turbulence. The height $y^+ \approx 100$ can be considered a lower bound for the logarithmic region, in the sense that the self-similarity of the velocity spectra, derived from the mixing length being proportional to y, does not hold below this height (Jiménez & Hoyas, 2008). By setting the boundary condition at this plane we avoid interfering with the log-layer dynamics.

Related to the studies of off-wall boundary conditions for LES is the investigation of Chapman & Kuhn (1986). Their study was an inverse use of approximate off-wall boundary conditions compared to those cited above. Rather than calculate the flow above the off-wall plane with LES, they carried out a Navier-Stokes calculation in the viscous sublayer below an off-wall plane by employing model boundary conditions there. These boundary conditions attempted to account for the magnitudes and phases of the velocity fluctuations at the off-wall plane with analytical functions constructed from what was known at the time from experiments about the structure of the flow above this plane. Ultimately, the goal was to provide physically accurate information in the near-wall layer that could be used for turbulence models in RANS calculations of bounded flows.

Pascarelli *et al.* (2000) addressed the need for greater resolution in the wall layer by using a so-called multi-block LES. The outer flow was computed with a lower-resolution grid in a flow domain block 1640 viscous lengths in width. The wall layer, where a higher-resolution grid was used and here bounded for the two cases studied by an upper plane at $y^+ = 30$ and 104 in a total computational domain 1230 viscous lengths high, was represented by two blocks of half the width of the outer layer, i.e., 820 viscous lengths. The width of these wall layer blocks was more than twice the domain width that Jiménez & Moin (1991) had determined is necessary to sustain turbulence in what they called the minimal flow unit in near-wall turbulence. The grid lines in the outer and inner layers of the study by Pascarelli *et al.* (2000) were continuous across the interface where information had to be exchanged. Although, as the authors state, the flow at the interface has a period set by the inner flow grid, they found that longer wavelengths occur within a few grid points from the interface. At much higher Reynolds numbers where the length scale separation within the inner and outer flows becomes much larger, many more repeated wall layer blocks can, of course, be used. First- and second-order statistics from the multi-block LES, when compared to a single-block calculation, showed good results for the wall layer block with its upper surface in the logarithmic layer at $y^+ = 104$. With this surface in the buffer layer at $y^+ = 30$, the Reynolds stresses were underpredicted and spurious pressure fluctuations occurred

The idea of simulating the overlying flow separately from the buffer layer, suggested by the work of Pascarelli *et al.* (2000) and some of the investigations cited above, can be pushed further by removing the buffer layer completely and modeling its effect on the rest of the flow as a boundary condition, imposed where the top of the buffer layer would be. This approach and a similar one have been tested in two recent studies. Podvin & Fraigneau (2011) generated synthetic boundary conditions from proper-orthogonal-decomposition eigenfunctions, which need to be obtained a priori. Mizuno & Jiménez (2013) constructed boundary conditions dynamically from information in the overlying flow, assuming that the turbulent fluctuations are self-similar across the log layer, and that this layer is essentially independent of the dynamics beneath.

Park *et al.* (2012) used the recent DNS by Wu & Moin (2010) of a spatially developing flat-plate boundary layer to obtain statistical properties of the turbulence in transition at $Re_\theta \approx 300$, from individual turbulent spots, and at $Re_\theta \approx 500$, where the spots merge (distributions of the mean velocity, Reynolds stresses, turbulent kinetic energy production and dissipation rates, enstrophy and its components), in order to compare to these statistical properties for the developed boundary layer turbulence at $Re_\theta = 1840$. When the distributions in the transitional regions were conditionally averaged so as to exclude locations and times when the flow is not turbulent, they closely resembled the distributions in the developed turbulent state at the higher Reynolds number, especially in the buffer layer and the viscous sublayer. Skin friction coefficients, determined in this conditional manner at the two Reynolds numbers in the transitional flow, are, of course, much larger than when their values are obtained by including both turbulent and non-turbulent information there, and the conditional averaged values are consistent with the 1/7th power law approximation. An octant analysis based on the combinations of signs of the velocity and temperature fluctuations, u, v and θ, showed that the momentum and heat fluxes are predominantly of the mean gradient type in both the transitional and developed regions. The fluxes appeared to be closely associated with vortices that transport momentum and heat toward and away from the wall in both regions of the flow. These results support the view that there is little difference between the structure and transport processes of a developed turbulent boundary layer and of turbulent spots that appear in transition.

The results of Park *et al.* (2012) motivated us to implement an off-wall boundary condition built from blocks of transitional wall layer flow. The blocks are taken from the turbulent spots that develop in the K-type transition case studied by Sayadi *et al.* (2012) in their spatially developing turbulent boundary layer DNS investigation. Our idea is to use space-time information from the turbulent spots of this simulation to develop a reduced-order, repeating pattern set of model off-wall boundary conditions for a full boundary layer LES.

The effect of the buffer layer is modeled as the imprint, at $y^+ \approx 100$, of a pattern of periodic blocks similar to the minimal unit of Jiménez & Moin (1991). This imprint is introduced as Dirichlet boundary conditions for the rest of the flow. The blocks are constructed from the transitional direct simulation of Sayadi *et al.* (2012). The block sizes are selected so that they are statistically representative of fully turbulent flow, and so that they contain the dominant structures at $y^+ \approx 100$, as educed from direct mode decomposition. The model has the form of a collection of Fourier modes in space and time, and comprises $\sim$1% of the parameters necessary to describe the full flow field at the plane considered, while it reproduces $\sim$90% of the amplitudes of the flow statistics.

The present work focuses on the synthesis of off-wall conditions and their implementation on fully resolved direct numerical simulations (DNSs). The treatment of subgrid-scale fluctuations at the boundaries and the application to LESs are left for future work.

IDENTIFICATION OF BLOCK UNITS

As stated above, our intention is to replace the viscous cycle of the turbulent structures with its imprint just below the beginning of the logarithmic region. So long as u_τ is uniform, as in channels and pipes, or varies slowly along the wall, as in boundary layers, we can conceive a model in which that imprint is formed by a pattern of quasi-periodic, repeating imprints from unit blocks submerged in the buffer layer. These blocks should be at least as large as the minimal flow unit in the buffer layer (Jiménez & Moin, 1991). If the incipient log-layer dynamics at $y^+ \approx 100$ are also to be taken into account, the blocks should be at least of length $L_x^+ \approx 600$ and span $L_z^+ \approx 300$ (Flores & Jiménez, 2010).

We compare results with models extracted from fully-developed channels and transitional boundary layers. The extraction of models from periodic channels is straightforward, using information from the full plane at $y^+ \approx 100$. In transitional flows, the selection of unit blocks is not inherent to the simulation domain, and deserves further discussion. In this case, the turbulence is not yet fully developed and exhibits a less chaotic behavior. The obvious advantage of using information from these regions is that temporal cycles can be more clearly identified, and a time-periodic behavior for our model can be more easily educed. The disadvantage is that the period of those cycles is extraneous to the dynamics of developed turbulence, since it is inherited from the instabilities that trigger transition. In K-type transition, for instance, the dominating frequency is the one associated with the excited Tollmien-Shlichting waves (Sayadi *et al.*, 2012). Nevertheless, these transitional regions represent the fully developed state relatively well, at least in a statistical sense (Park *et al.*, 2012). We have focused on the K-type transitional boundary layer of Sayadi *et al.* (2012) because, in this flow, the turbulent spots are pinned to well-delimited locations, i.e., the paths of the wakes of the lambda vortices generated by the excitation of the Tollmien-Schlichting modes. Blocks bounded by the wall and $y^+ = 100$ can then be defined at locations fixed in space, and data from the flow that passes through the blocks can be collected to construct our reduced-order, repeated-pattern, off-wall boundary models. To determine the optimum size of the unit blocks for our model, we have used three different criteria, which are detailed below. We have looked for compromise solutions that satisfied simultaneously the three criteria reasonably well.

Statistical criteria

An adequate model should at least reproduce the corresponding real flow in a statistical sense, so we first compare the statistical properties of the flow within the block to those of fully developed turbulence. Park *et al.* (2012) proposed a method to identify turbulent spots from a threshold in the enstrophy within the buffer layer, and also at the first point away from the solid wall. The latter threshold criterion is equivalent to classifying the wall friction as laminar or turbulent. We use an analogous criterion to select the streamwise and spanwise dimensions of our candidate blocks. We

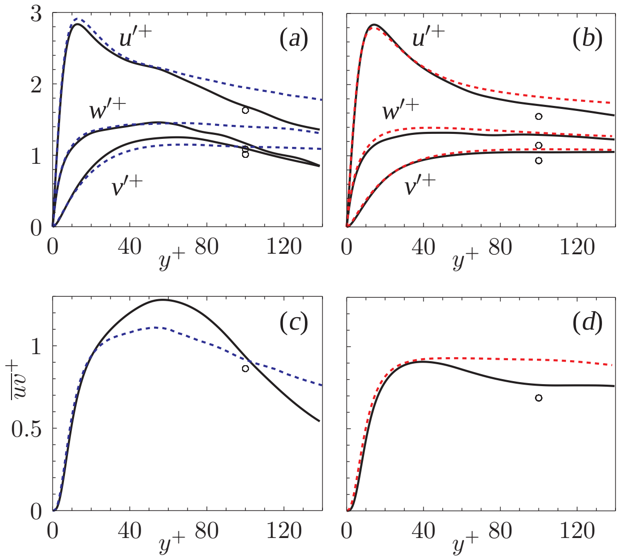

Figure 1. Flow statistics from transitional boundary layer blocks, (*a*) and (*c*) at $Re_\theta \approx 510$, and (*b*) and (*d*) at $Re_\theta \approx 1300$. (*a*) and (*b*), rms velocity fluctuations. (*c*) and (*d*), *uv* Reynolds shear stress. ----, results from Park *et al.* (2012); ——, data from the present optimal blocks; ○, data from the reduced-order model.

analyze the dependence on the block dimensions of the local friction coefficient, $c_f = 2/(U_\infty^+)^2$, evaluated only for the portion of the wall beneath the block. The idea is to select the block size so that c_f is as close as possible to the fully turbulent one. We have evaluated c_f at two stages in transition, with $Re_\theta \approx 510$ and $Re_\theta \approx 1300$. In both cases, the value of c_f is moderately sensitive to the spanwise size of the block, L_z^+, and relatively insensitive to the streamwise one, L_x^+. The reason for the spanwise sensitivity is that the flow is well organized, and the mean local friction varies greatly, depending on whether it is measured inside or outside of the wake of the Tollmien-Schlichting-triggered turbulent patches. Blocks with $L_z^+ \approx 100$ include only a region within a train of horseshoe vortices, which is in essence a low-speed streak, resulting in significantly lower c_f. On the other hand, the sensitivity of c_f to L_x^+ is rather small because, during a full time period of the Tollmien-Schlichting wave, a given x location experiences a full streamwise cycle of the flow oscillations as the flow is advected downstream, and all the information from a full cycle can be captured at a single x station reasonably well. This would be a common feature of any quasi-periodic flow advected at a roughly constant velocity for which the streamwise coordinate and the time are essentially interchangeable. Notice that in a non-deterministic type of wall turbulence, like channels or fully developed boundary layers, different events would not have a preferential location in x or z. The blocks could then be chosen of any arbitrary size, and, given enough time, their statistics would converge to those of the full flow, so a statistical criterion would not be useful to determine the adequate size of the unit block. In our case, while the optimum L_z^+ can be determined simply from such a criterion, the determination of L_x^+ requires additional information.

We also verify that other flow statistics do not deviate significantly from the fully developed ones. As in Park *et al.* (2012), we collect mean profile and fluctuation statistics for the velocities, restricted within the block and normalized with the mean wall shear stress associated with c_f as defined above. We also collect statistics for the uv Reynolds stress in the same fashion. As for c_f, we compare the statistics thus obtained with those of the fully developed flow at a roughly equal Re_θ, and check that their differences remain small, particularly at $y^+ \approx 100$. The results for the optimal blocks are shown in Figure 1. Since the block at $\mathrm{Re}_\theta \approx 510$ is in a more incipient state of turbulence, its statistical properties deviate somewhat more significantly from the fully turbulent regime than those at $\mathrm{Re}_\theta \approx 1300$. The friction Reynolds number calculated strictly within the first block, $\mathrm{Re}_\tau \approx 125$, is also slightly lower than that of Park *et al.* (2012) at $\mathrm{Re}_\theta \approx 500$. At the same time, the flow is simpler there than farther downstream, and exhibits little randomness, making it more suitable for model reduction. The block at $\mathrm{Re}_\theta \approx 1300$, on the other hand, exhibits a more turbulent behavior, but the increased chaos makes the identification of dominating patterns more subtle.

Spectral criteria

The fact that correct statistics can be obtained from blocks with unsuitable dimensions, for sufficiently disorganized turbulence, illustrates how statistical resemblance cannot be the only criterion to select the block size. Information on the length scales of the dominant structures must also be considered. Statistically, the length scales of the most energetic structures can be identified from the regions of high concentration in the premultiplied spectral energy density maps $k_x k_z E_{uu}$ of the flow variables. We have analyzed these maps, calculated from data within our unit blocks, for the three velocity components, verifying that the energy is concentrated in wavelength ranges contained within the blocks. In the case of u, structures elongated in the streamwise direction, of the size of the block or longer, have significant energy, and the model will reproduce very elongated structures as constant in x. Note that the concentration of energy at the longest wavelengths is present even for the largest domains at which channel DNSs have been conducted (Jiménez & Hoyas, 2008).

Dynamic Mode Decomposition

Dynamic Mode Decomposition (Schmid, 2010) has recently been proposed as a technique to capture coherent features in both experimental and numerical flows. DMD can extract, directly from a collection of flow field snapshots, the most significant coherent modes of the flow. The method can extract dynamic information, such as phase velocities, which are not available with other methods such as Proper Orthogonal Decomposition. Direct modes can be interpreted as a generalization of global stability modes, and are also associated with eigenvalues with real and imaginary parts, i.e., they have amplification rates and phase velocities.

We have applied DMD to the three velocity components within our unit blocks, with mixed results. While we have not been able to produce efficient models through DMD per se, we have found it to provide vital information to select the correct block size for those models. One of the problems for efficient model reduction is that, because of the partly chaotic nature of wall turbulence, only a small number of the dynamic modes obtained can be dropped if one is to obtain a good representation of the flow. Furthermore, the modes identified by DMD have either positive or negative, but strictly non-zero, growth rates. The amplitude of the modes is then not significant during the whole interval on which they are extracted, and they either decay soon or become important late, so that only the full collection can capture the main features of the flow during the complete interval sampled. If the modal decomposition is extrapolated to times beyond that interval, only modes with positive amplification survive, and they eventually diverge, so the extension in time for model construction requires additional care.

On the other hand, DMD provides very useful information on the spatial coherence of the flow. The resulting modes exhibit very clear spatial wavelengths that need not be harmonics of the dimensions of the subdomain on which DMD is applied. Thus, DMD can be carried out in regions sufficiently larger than the optimal block, providing information on the largest wavelengths of the coherent features. Blocks smaller than those wavelengths would not contain the coherent structures fully, and larger ones would contain an unnecessary repetition of them. We can use that information to select the size of the unit block in our model. In particular, we have used this property to determine L_x^+, and to finely adjust the value of L_z^+. For the full collection of modes, the dimension of the optimum block is the least common multiple of the wavelengths of all the modes.

REDUCED-ORDER MODEL FROM FOURIER MODAL ANALYSIS

Once we have selected an appropriate buffer layer unit block, we need to extract an adequate boundary condition from it. Our intention is to represent the velocity field at the selected boundary plane with the least possible number of parameters. For that, we consider the time-resolved flow variables only at $y^+ \approx 100$ and within the block. The model is designed to be periodic in the streamwise and spanwise directions, by repetition of the unit block upper plane, but also periodic in time, so Fourier decomposition both in space and time, followed by truncation, emerges as a natural method. Note that such a model imposes a specific set of wavelengths at the boundary plane, and forces the rest to be zero. If the plane contains, for example, two blocks in x, only even k_x modes would be non-zero. Although this wavelength selection is artificial, it has been shown to reproduce the characteristics of turbulence reasonably well (Pascarelli *et al.*, 2000; Mizuno & Jiménez, 2013).

Fourier decomposition assumes that any flow variable ϕ at $y^+ \approx 100$ is periodic in the unit block and in the time interval considered, so that it can be expressed as $\phi(x,z,t) = \sum_{k_x,k_z,\omega_t} \widehat{\phi}_{k_x,k_z,\omega_t} \mathrm{e}^{-\mathrm{i}(k_x x + k_z z + \omega_t t)}$. The decomposition in time is carried out taking 50 snapshots that cover a full Tollmien-Schlichting period. Since the eigenmodes $\widehat{\phi}_{k_x,k_z,\omega_t}$ are orthogonal, the total energy ϕ^2 can be obtained from the sum of $\widehat{\phi}^2_{k_x,k_z,\omega_t}$. This provides a criterion to sort the eigenmodes, selecting the most energetically significant ones. We have followed that criterion to generate our reduced-order model. When the modes are sorted according to the energy in the three velocity components, modes beyond the first $\sim$1000 have energies $\sim$3 orders of magnitude smaller than the most significant mode. We truncate our model to the first 2000 modes. The energy they contain is, for each velocity fluctuation, roughly 90% of the total, as shown in Figure 1. The error in the resulting Reynolds shear stress is of the same order. Notice that selecting 2000 modes can thought of as selecting roughly 12 streamwise wavelengths, 12 spanwise wavelengths, and 12 frequencies in time. That represents roughly 2% of the total number of modes $\widehat{\phi}_{k_x,k_z,\omega_t}$ available.

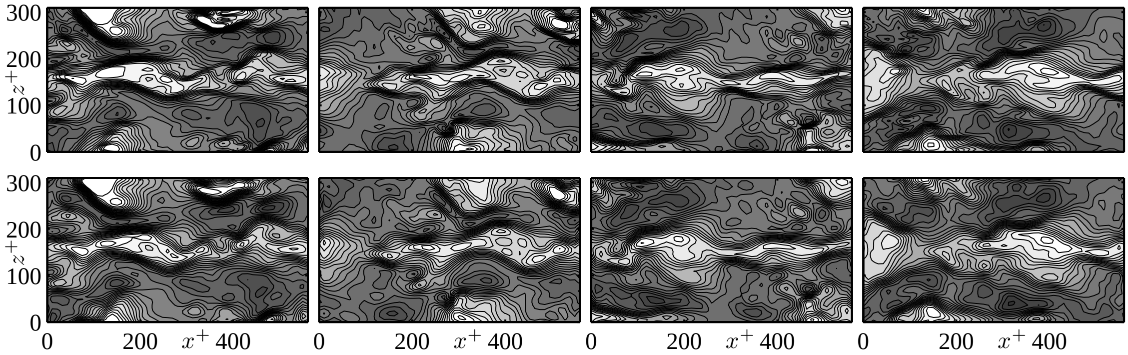

Figure 2. Instantaneous realizations of u at $y^+ \approx 100$, in the unit block at $\mathrm{Re}_\theta \approx 510$. Top, DNS data from Sayadi *et al.* (2012). Bottom, present reduced order model. From left to right, instantaneous captures at consecutive quarters of a Tollmien-Schlichting cycle.

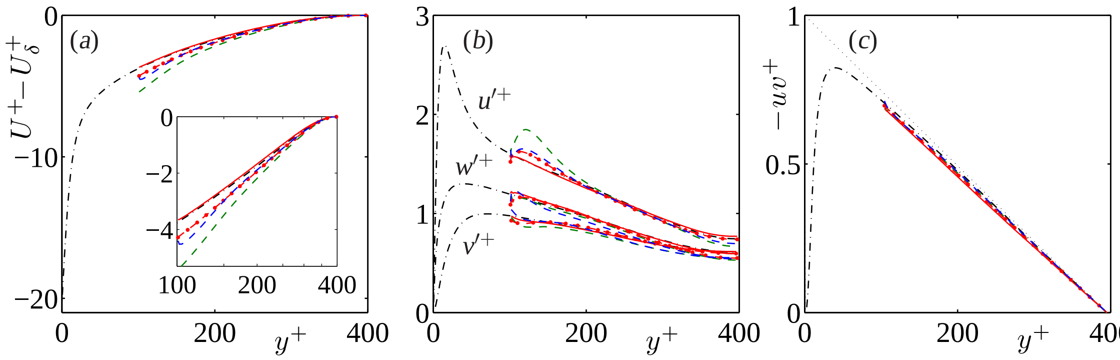

Figure 3. Flow statistics from the present channel flow simulations at $\mathrm{Re}_\tau \approx 395$. (*a*) mean velocity profile; (*b*) rms velocity fluctuations; (*c*) Reynolds shear stress. — · — , full-channel DNS; ———, off-wall exact boundary conditions; •••••, reduced-order modeled boundary conditions obtained from the exact ones; - - - -, lattice, reduced-order, modeled boundary conditions obtained from a 'minimal' channel DNS; - - - -, reduced-order conditions from the transitional boundary layer of Sayadi *et al.* (2012), unit block at $\mathrm{Re}_\theta \approx 500$; - - - -, idem, at $\mathrm{Re}_\theta \approx 1300$.

The chosen modes can be stored in Fourier space in compact form, easily accessible by simulations with model boundaries. The simulations reconstruct the time-resolved boundary conditions through inverse Fourier transforms. Figure 2 portrays a reconstruction for the u field at different times of the Tollmien-Schlichting cycle, compared with the original signal. The reconstruction procedure results in a representation in which the dominant, energy-carrying structures are present, although some minor or short-lived features are missing.

IMPLEMENTATION FOR CHANNEL FLOW

As a first benchmark case for our off-wall boundary conditions, we select a turbulent channel at $\mathrm{Re}_\tau = 395$, with DNS resolution. This is a particularly simple case because of its homogeneity in the wall-parallel directions. For a boundary layer, for instance, the effect of streamwise evolution should be taken into account, modulating the boundary condition. In the case of channels, the boundary condition can be imposed in a uniform lattice without any further considerations.

We have used the incompressible, fractional-step channel code of Bose *et al.* (2010), adapting it to allow for non-zero, off-wall boundary conditions. The code uses a finite-difference discretization in space with grid stretching in the wall-normal direction, and a Runge-Kutta/Crank-Nicholson scheme in time. The doubly periodic domain size is $2.15\pi\delta \times 2\delta \times 0.97\delta$, adjusted so that a lattice of exactly 3×3 unit blocks can be imposed at the off-wall boundary plane. The grid size is $384 \times 350 \times 384$ for the full channel, resulting in a resolution $\Delta x^+ \approx 7$, $\Delta y^+ \approx 0.3$ near the wall and ≈ 5 at the channel center, and $\Delta z^+ \approx 3$. In the off-wall boundary simulations, only the central 158 wall-parallel planes were solved for, with the minimum Δy^+ being then ≈ 2.3.

Using this code we have conducted a set of simulations in which the different levels of abstraction in our model were introduced progressively. First, a full DNS of the whole channel was conducted, and the time histories of the flow velocities at the designated $y^+ \approx 100$ planes were saved. In a second simulation, starting from the same initial condition, those time histories were implemented as 'exact' off-wall boundary conditions. The same histories were also used to synthesize reduced-order boundary conditions, but only through Fourier transform followed by truncation. In the next step, the modeled boundary conditions were synthesized from the DNS of a channel at the same Re_τ but with $1/3$ streamwise and spanwise box lengths, close to the minimal unit of Jiménez & Moin (1991). Finally, the modeled conditions obtained from the transitional boundary layer of Sayadi *et al.* (2012) were implemented.

The resulting velocity statistics are portrayed in Figure 3, including the mean velocity profiles, the fluctuation rms values for the three velocity components, and the Reynolds shear stress. The results with off-wall boundary conditions are in very good agreement with those of the full channel, except perhaps in a thin layer near the boundary plane, where mild kinks in the velocity fluctuations appear. Those kinks are present even for 'exact' boundary conditions, for which they grow in intensity with time, although the time span considered for the statistics in that case, $\sim 5\delta/u_\tau$, was too short for the kinks to be noticeable in the figure. Similar kinks appeared in simulations with off-wall boundaries by other authors, namely Podvin & Fraigneau (2011), Mizuno & Jiménez (2013), and even in the inverse case, simulating the flow between the wall and the off-wall plane, of Chapman & Kuhn (1986). Both Podvin & Fraigneau (2011) and Mizuno & Jiménez (2013) argued that the appearance of these kinks is due to the decoupling of the boundary condition and the overlying flow, so that the flow requires an adjustment region to adapt to the prescribed boundary values. In our simulations, the intensity of the kinks seems to increase as more layers of abstraction are added to the boundary condition. Nevertheless, the agreement with full-channel results is remarkable, particularly in the case of boundary conditions from transitional boundary layer data, considering they are obtained from an entirely different flow. The most noticeable difference is probably the mismatch in the mean velocity profile. This mismatch is due to the very small relative differences in the Reynolds stress. Since the Reynolds and viscous stresses must sum up to the same, linear-with-y total stress, and the viscous stress is much smaller than the Reynolds one in the channel core, the small relative error in the latter translates into a larger relative error in the former. This larger error in viscous stress is in fact a larger error in the slope of the mean velocity profile. Nevertheless, even if the mismatch in the profile is substantially larger for the boundary condition derived from boundary-layer data, it is still of order $\Delta U^+ \approx 1$ at most, which is $\sim 5\%$ of the centerline velocity.

CONCLUSIONS AND FUTURE WORK

In the present work, we propose a novel set of off-wall boundary conditions for the outer flow, to overcome the need to fully resolve the scales of motion in the near-wall layer. We have presented a reduced-order model consisting of a pattern of periodic blocks, representing the effect of the buffer layer on the outer flow. The unit blocks have been obtained from fully turbulent channel flow and from the DNS of Sayadi *et al.* (2012) for a K-type transitional boundary layer. The block size is selected so that it represents the near-wall flow both statistically and structurally. Once the block is selected, we educe a simplified flow field at a plane $y^+ \approx 100$ by Fourier decomposition and truncation, both in space and time. That flow field can then be replicated in a repeating pattern and supplied as a boundary condition for an independent simulation of the outer turbulence. We have tested this model on turbulent channel flow, obtaining good agreement with the statistics from full channel DNS.

Once the model is completely set up, the next step in the project will be adapting it for LES, determining which components of the boundary conditions should act on the resolved scales and which on the subgrid ones. The model will also need to react to the fluctuations of the larger, inactive scales, and to inhomogeneities in the wall-parallel plane, first so they can be applied to smooth-wall, zero-pressure-gradient boundary layers, and later to more complex geometries.

REFERENCES

Bagwell, T., Adrian, R., Moser, R. & Kim, J. 1993 Improved approximation of wall shear stress boundary conditions for large eddy simulation. In *Near-Wall Turbulent Flows* (ed. R. So, C. Speziale & B. Lauder), pp. 265–276. New York: Elsevier Science.

Balaras, E., Benocci, C. & Piomelli, U. 1996 Two-layer approximate boundary conditions for large-eddy simulations. *AIAA J.* **34**, 1111–1119.

Bose, S. T., Moin, P. & You, D. 2010 Grid-independent large-eddy simulation using explicit filtering. *Phys. Fluids* **22**, 105103.

Cabot, W. & Moin, P. 1999 Approximate wall boundary conditions in the large eddy simulation of high Reynolds number flow. *Flow, Turb. and Comb.* **63**, 269–291.

Chapman, D. & Kuhn, G. 1986 The limiting behavior of turbulence near a wall. *J. Fluid Mech.* **170**, 265–292.

Chung, D. & Pullin, D. 2009 Large-eddy simulation and wall modelling of turbulent channel flow. *J. Fluid Mech.* **631**, 281–309.

Flores, O. & Jiménez, J. 2010 Hierarchy of minimal flow units in the logarithmic layer. *Phys. Fluids* **22**, 071704.

Jiménez, J. & Hoyas, S. 2008 Turbulent fluctuations above the buffer layer of wall-bounded flows. *J. Fluid Mech.* **611**, 215–236.

Jiménez, J. & Moin, P. 1991 The minimal flow unit in near-wall turbulence. *J. Fluid Mech.* **225**, 213–240.

Jiménez, J. & Vasco, C. 1998 Approximate lateral boundary conditions for turbulent simulations. In *Studying turbulence using numerical simualtion* (ed. P. Moin & W. Reynolds), pp. 399–412. Stanford, CA: Center for Turbulence Research.

Mizuno, Y. & Jiménez, J. 2013 Wall turbulence without walls. *J. Fluid Mech.* **723**, 429–455.

Nicoud, F., Winklemans, G., Carati, D., Baggett, J. & Cabot, W. 1998 Boundary conditions for LES away from the wall. In *Studying turbulence using numerical simulation* (ed. P. Moin & W. Reynolds), pp. 413–422. Stanford, CA: Center for Turbulence Research.

Park, G., Wallace, J., Wu, X. & Moin, P. 2012 Boundary layer turbulence in transitional and developed states. *Phys. Fluids* **24**, 035105.

Pascarelli, A., Piomelli, U. & Candler, G. 2000 Multi-block large-eddy simulations of turbulent boundary layers. *J. Comp. Phys.* **157**, 256–279.

Piomelli, U. & Balaras, E. 2002 Wall-layer models for large-eddy simulations. *Annu. Rev. Fluid Mech.* **34**, 349–374.

Podvin, B. & Fraigneau, Y. 2011 Synthetic wall boundary conditions for the direct numerical simulation of wall-bounded turbulence. *J. Turbulence* **12**, 1–26.

Sayadi, T., Hamman, C. & Moin, P. 2012 Direct numerical simulation of complete transition to turbulence via h-type and k-type secondary mechanisms. *Submitted* .

Schmid, P. J. 2010 Dynamic mode decomposition of numerical and experimental data. *J. Fluid Mech.* **656**, 5–28.

Wu, X. & Moin, P. 2010 Transitional and turbulent boundary layer with heat transfer. *Phys. Fluids* **22**, 085105.